INFLUENCE OF REINFORCEMENT MATERIALS ON EXPLOSION RESISTANCE OF CARBON FIBER REINFORCED PLASTIC

A.I. Dulnev[1], E.A. Nekliudova[2]

[1] Krylov State Research Centre, St. Petersburg, Russia
Email: A_Dulnev@ksrc.ru, Web Page: http://www.krylov-center.ru
[2] Krylov State Research Centre, St. Petersburg, Russia
Email: ekaterina.nekliudova@yandex.ru, Web Page: http://www.krylov-center.ru

Keywords: carbon fiber reinforced plastic, underwater explosion, fiber rupture, through-thickness penetration

Abstract
This paper presents the results obtained from a computational- cum-experimental investigation into resistance of carbon fiber plastic samples to non-contact underwater explosion (UNDEX). Tests were carried out on three groups of samples manufactured using different reinforcement materials. The layup patterns provided quasi-isotropic properties of the material. The test samples were shaped as circular plates. The tests were performed in an explosion chamber using a so-called water-air setup. The sample damage was assessed versus two indicators (criteria): 1 - rupture of individual fibers and 2 - through-thickness penetration (hole). It is experimentally demonstrated that quadraxial carbon fabric samples show the best explosion resistance versus through-thickness penetration criterion due to better deformation characteristics as well higher interlaminar shear strength of the quadraxial carbon fiber plastic as compared with other materials under study. Based on the analysis of computational and experimental data it is demonstrated that by the moment when fibers start to rupture the equivalent strains in the middle of the test material samples, which have approximately the same ultimate tensile strength in different directions, show good correlation with the tensile elongation found in static tests.

1. Introduction

Structural materials are exposed to a wide spectrum of loads in the service life of constructions, including strong dynamic impacts caused by explosions. In the recent years polymer composite materials, in particular glass- and carbon-fiber reinforced plastics, have been increasingly used as structural materials in various fields of engineering. Resistance of these materials to loads strongly depends on the reinforcement materials, binders, reinforcement patterns, manufacturing processes, etc. The resistance of polymer composite materials (PCM) has been widely discussed primarily in the context of static and quasi-static loading, while much less attention is paid to explosion-induced effects, in particular, underwater explosions (UNDEX). However, such investigations should be of interest for the choice of the best PCM options for prospective applications.

Most of the published papers on the PCM resistance to underwater explosions focus on glass fiber plastics (see [1-5], etc.). Much less attention has been paid to investigation of carbon fiber reinforced plastics (CFRP) in this respect. Some aspects of CFRP resistance to UNDEX were considered, for example, in [6, 7]. The explosion resistance of CFRP and GRP were compared, for example, in [8].

The main purposes of this study were

- to obtain experimental data for evaluating the size and pattern of damage in CFRP test samples versus explosion load parameters;
- to assess the explosion resistance of CFRP samples made with different reinforcement materials;

- to elaborate computer models and use computer simulation techniques for analysis of the stress-strain state of test samples as applied to given test conditions.

2. Test materials and samples

Tests were carried out on three groups of samples manufactured using different reinforcement materials:

- twilled carbon fabric (layup 0°/90°) and biaxial diagonal carbon fabric (layup +45°/-45°); bag layup pattern $[(0°/90°)_2/(+45°/-45°)_1/\ldots/(+45°/-45°)_1/(0°/90°)_2]$ – group 1;
- biaxial carbon fabric (layup 0°/90°) and biaxial diagonal carbon fabric (layup +45°/-45°); bag layup pattern $[(0°/90°)_2/(+45°/-45°)_1/\ldots/(+45°/-45°)_1/(0°/90°)_2]$ – group 2;
- quadraxial carbon fabrics; bag layup pattern [0°/+45°/90°/-45°] – group 3.

The samples were made by vacuum infusion process using a vinyl ester binder. Table 1 gives characteristics of the sample groups. The main mechanical characteristics of CFRPs under study are shown in Table 2. The bag layup pattern provided quasi-isotropic properties of the material. Sample cutting directions are indicated in Table 2 as follows: X_1 and X_2 – along fibers in reinforcement plane 12; X_{12} – at 45^0 to X_1 and X_2 direction in reinforcement plane 12; X_3 – perpendicular to reinforcement plane plane 12.

Table 1. Main characteristics of test samples

Sample group	Number of samples	Thickness, δ, mm	Density, ρ, kg/m^3	Surface mass, m, kg/m^2	Number of layers
1	4	5.85-5.94	1503-1526	8.93	14+6
	4	5.16-5.1	1519-1532	7.91	12+6
2	4	5.73-5.76	1493-1500	8.60	7+6
3	4	5.28-5.37	1551-1577	8.33	7

Table 2. Main mechanical characteristics of CFRPs

Characteristics	Direction	Group 1	Group 2	Group 3
Modulus of elasticity, GPa	X_1	50.8	50.0	42.4
	X_{12}	33.2	37.5	45.6
	X_2	50.0	55.3	47
Modulus of shear in reinforcement plane, GPa	X_1	14.0	11.5	9.25
	X_{12}	7.83	6.85	9.59
	X_2	14.90	11.2	-
Modulus of interlaminar shear, GPa	X_1	2.77	3.03	4.49
	X_2	2.70	3.13	4.17
Poisson ratio in plane 12	-	0.27	0.27	0.32
Ultimate tensile elongation, %	X_1	1.09	1.98	1.92
	X_{12}	1.96	1.85	1.74
	X_2	1.22	1.94	1.9
Ultimate tensile/compressive strength, MPa	X_1	568/350	993/372	778/372
	X_{12}	574/315	619/359	752/372
	X_2	607/278	1076/414	866/387
Ultimate interlaminar shear strength, MPa	X_1	44.1	40	55.2
	X_{12}	37.6	48	55.8
	X_2	38	42	57.2

The samples were circular plates with a radius of 400 mm. Each plate had 18 holes for bolts. Bolt setting radius was 250 mm. Samples were made with a circular mould-on portion in way of the bolt joints to achieve identical failure patterns, i.e. to obtain damage (fiber rupture, penetration hole) in the middle of the sample and avoid any fractures at supports or near bolt joints, which are treated as accidental and largely dependent on the sample fixing arrangements. Total thickness at the mould-on portion was 14 mm.

3. Experimental set-up

The samples were tested in the explosion chamber of Krylov State Research Centre. The schematic arrangement of this facility is shown in Fig. 1a. The tests were performed using a so-called water-air set-up when the sample facing the explosion was backed by air-filled space. Each sample was exposed to one explosion. Every time an explosive charge was placed vis-a-vis the sample center at a fixed distance (300 mm), the charge mass Q was varied (from 20 to 50 g). The charge itself was a plastic explosive of cylinder shape with a height to diameter ratio of 1. TNT equivalent in terms of the specific blast energy was ~ 1.

Fig. 1b shows the test dummy assembly. The sample was fixed with 18 bolts between the matrix foundation (tubing) and clamping metal strip (ring). A rubber gasket was fitted between the clamp and the sample to seal the assembly. The effective test field diameter of the matrix-mounted sample was 400 mm. The test assembly was suspended vertically in the explosion chamber, which was filled with water so that the water surface was at least 1.0 m above the top of the assembly.

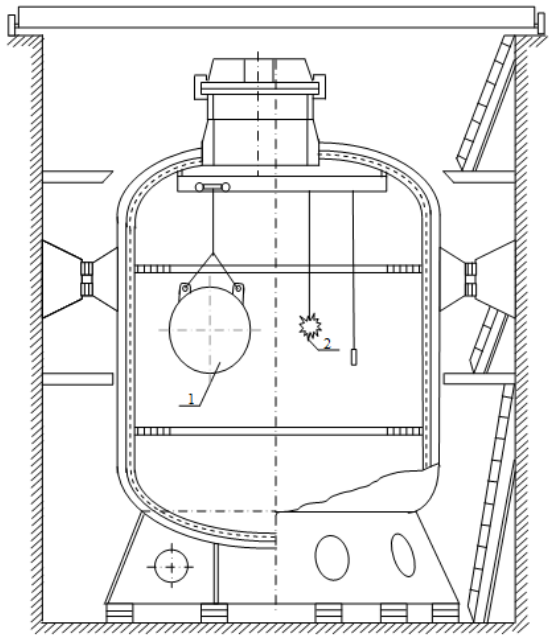

a) Explosion chamber:
1 – dummy, 2 – charge

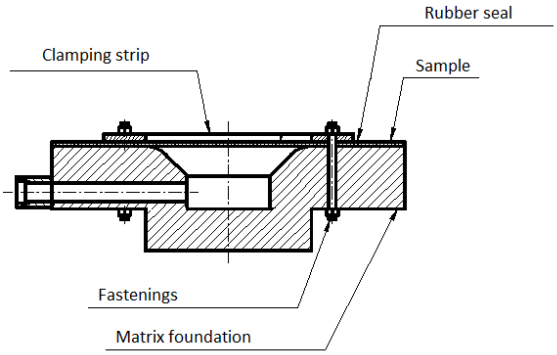

b) Dummy assembly

Figure 1. Explosion chamber and dummy assembly.

During the tests the strains at the back side of the sample (i.e. on the opposite side to the explosion) were recorded. Strain gauges to record radial and circular strains were fitted at different points around the sample r=110-125 mm (Fig. 2). Some strain gages were duplicated for redundancy.

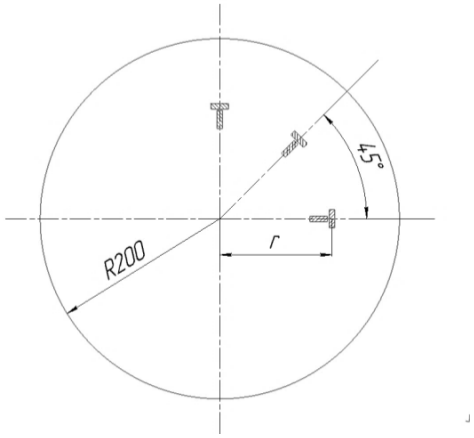

Figure 2. Arrangement of the strain gauges on the samples.

Based on the test data, different amount of damage inflicted on samples in each test group were correlated with the mass of explosive charges. The amount of damage was assessed versus two indicators (criteria): 1 – rupture of individual fibers; 2 – through-thickness penetration (hole). In accordance with the said criteria two levels of explosion resistance were established for the test samples. To generalize the test results obtained for the samples with different surface masses, a measure of the explosion effect was introduced: relative charge mass $\beta = m_{ex} / m$, where m_{ex} is the mass of charge per unit of the sample's test area, kg/m^2; m – surface mass of the sample, kg/m^2. Thus, the relative charge mass triggering one or another kind of damage is taken as a measure of specific explosion resistance of the samples.

4. Test results

Fig. 3 - 5 show photos of typical failure patterns of samples, and Table 3 contains the relative masses of charges obtained from test data analysis to characterize different explosion resistance levels of samples.

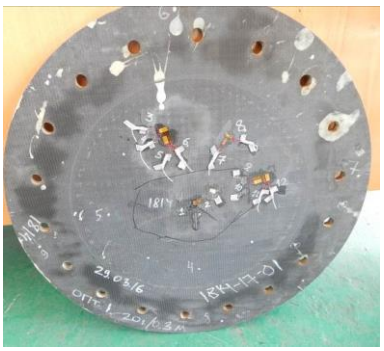

a) fiber rupture in the first layer, at the back side (Q=20 g, β=1.78 %, δ=5.94 mm, m=8.93 kg/m^2)

b) fiber rupture in several layers, at the back side (Q=30 g, β=3.01 %, δ=5.21 mm, m=7.91 kg/m^2)

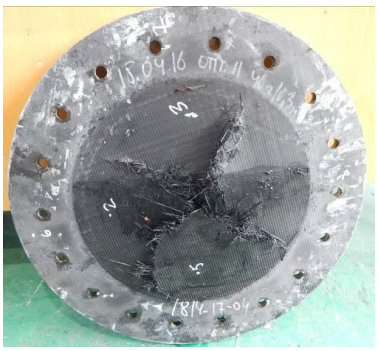

c) penetration hole, back side (Q=40 g, β=3.55 %, δ=5.88 mm, m=8,93 kg/m^2)

Figure 3. Typical damage patterns of group 1 samples.

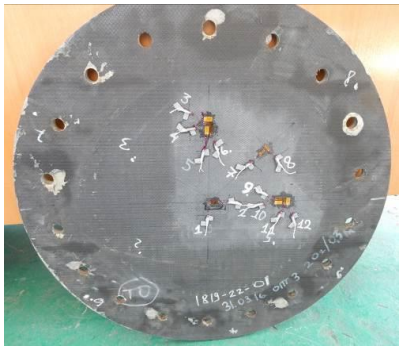

a) fiber rupture in the first layer, at the back side (Q=20 g, β=1.84 %, δ=5.75 mm, m=8.60 kg/m^2)

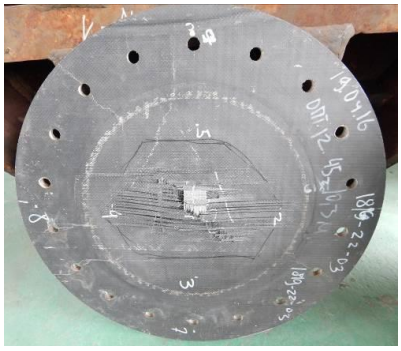

b) fiber rupture in several layers, at the back side (Q=45 g, β=4.15 %, δ=5.76 mm, m=8.60 kg/m^2)

c) penetration hole, back side (Q=50 g, β=4.61 %, δ=5.73 mm, m=8.60 kg/m^2)

Figure 4. Typical damage patterns of group 2 samples.

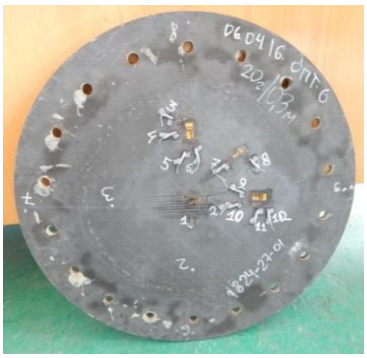

a) fiber rupture in two layers, at the back side (Q=20 g, β=1.90 %, δ=5.28 mm, m=8.33 kg/m^2)

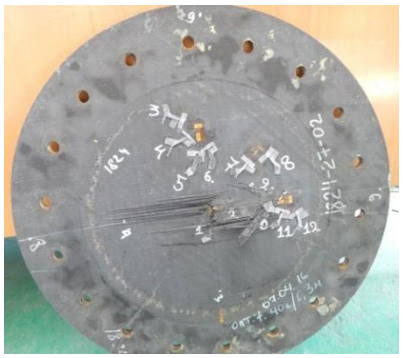

b) fiber rupture in several layers, at the back side (Q=40 g, β=3.81 %, δ=5.29 mm, m=8.33 kg/m^2)

c) damage at mould-on portion, face side (Q=50 g, β=4.76 %, δ=5.37 mm, m=8.33 kg/m^2)

Figure 5. Typical damage patterns of group 3 samples.

Table 3. Explosion resistance of CFRP test sample groups.

Sample group No.	Surface mass, kg/m^2	Relative charge mass β for various explosion resistance levels,%	
		β_1	β_2
1	8.93 7.91	≤1.78	≈3.29
2	8.60	≈1.84	≈4.34
3	8.33	≤1.90	>4.76

As the explosion power (charge mass) is progressively increased it is seen that binders of test samples start to fail, first in the center and in the supported portion of a sample, then this damage spreads over the entire test area of the sample. It follows by rupture of individual carbon fibers in the middle part, starting from the back layer (Figs 3a, 4a, 5a). At this stage the rupture of fibers is mostly chaotic. Gradually, the number of layers with ruptured fibers in the middle is growing (Figs 3b, 4b, 5b). At this stage it is noted that two main intersecting cracks/fractures are initiated in the samples of group 1 (Fig. 3b). At the same time, the samples of groups 2 and 3 show multiple fiber ruptures in one direction (Figs 4b and 5b). Finally a through-thickness penetration hole is formed (Figs 3c and 4c). The penetration hole of group 3 samples was not obtained in the middle, but occurred in way of the support, at the mould-on portion.

In general, the test results indicate that:

- CFRP samples of groups 2 and 3 have approximately the same explosion resistance up to the fiber rupture initiation, which is primarily related to the ultimate tensile elongation of the CFRPs under consideration (see Table 2) : for group 2 ε_1=1.98 %, ε_2=1.94 %, ε_{12}=1,74 %, while for group 3 ε_1=1.92 %, ε_2=1.9 %, ε_{12}=1,85 %;
- Quadraxial CFRP samples (group 3) show the highest resistance in terms of the penetration hole criterion; the lowest resistance in terms of this criterion is shown by twilled carbon fabric and biaxial diagonal carbon fabric (group 1).

From comparison of the mechanical characteristics of group 2 and 3 samples (see Table 2), it is seen that these groups have approximately the same ultimate tensile strength and strain characteristics. However, group 3 has a significantly higher interlaminar shear limit. In this connection, it can be assumed that the higher explosion resistance of group 3 samples up to the occurrence of penetration hole is related to this material characteristic.

Fig. 6 presents characteristic time histories of strains for the test samples at β=1.78 % (Q=20 g, δ=5.94 mm) – group 1, β=1.84 % (Q=20 g, δ=5.75 mm) – group 2 and β=1.90 % (Q=20 g, δ=5.28 mm) – group 3. The figure shows averaged curves based on readings of 3 to 5 strain gauges fitted circumferentially over a circle r (see Fig. 2).

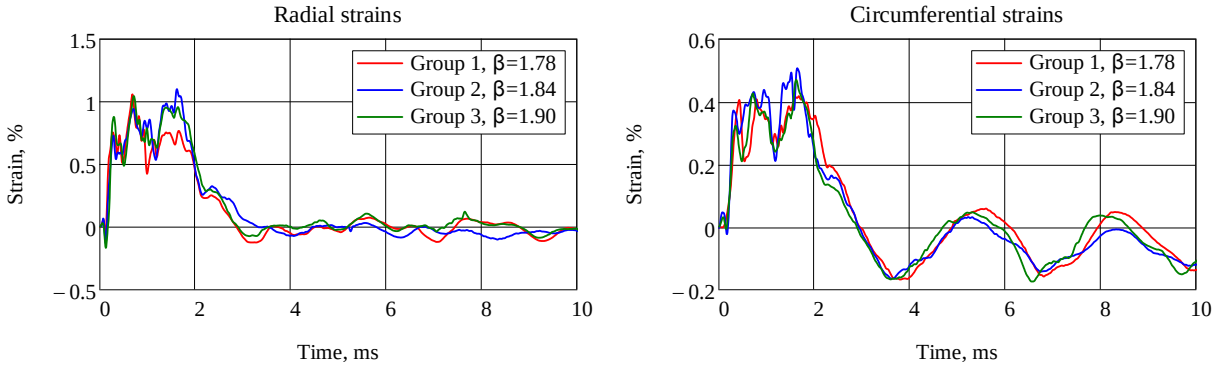

Figure 6. Strain versus time.

Regarding the strain measurements the following should be noted. There is a transitory process of sample deformation before initiation of fiber rupture lasting 3 ms. This time depends among other factors on sample frequency responses. The maximum radial strains at the measurement points are ~2-2.5 times higher than the circumferential strains. The maximum radial strains at the measurement points reach about 1 %. This value is higher in the middle of test samples and approximately corresponds to the tensile elongation of these materials. The strain measurements were used for verification of computation models.

5. Computer simulation of stress-strain states for test samples

The purpose of the computer-based simulation was to develop analytical FEM-based models for adequate prediction of strain behavior for test samples exposed to UNDEX. The necessity to apply computer-based models in stress-strain analysis is required, among other reasons, due to limited availability of experimental sample strain data. In particular, when the explosion occurs near the sample, strains are practically impossible to record on the front side of the sample, and even on its back side at the center of the sample.

Considering that the processes invoked by a proximity non-contact UNDEX are quite complicated, the test conditions were simulated using two FEM-based programs: LS-DYNA and AUTODYN. The formulation of the problem was three-dimensional in both cases. Since the samples were symmetric, only a quarter of the test area was simulated: a segment of fluid (water) with radius of 660-900 mm and height of 810-1050 mm with the cut-out in the upper part running along the contour, its size being equal to overall dimensions of the tubing (see Fig. 7). The sample was put inside the cut-out, and above the sample, there was air-filled space corresponding to the free volume in the tubing behind the sample. The design diameter of the sample was assumed as equal to the bolt joint diameter, i.e. 500 mm.

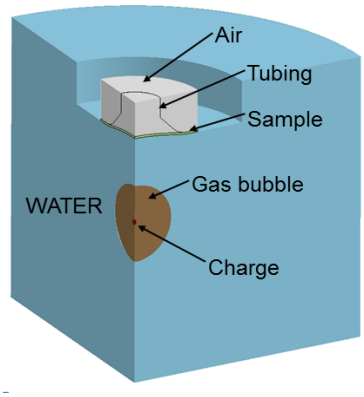

Figure 7. Computational domain in the test simulation.

Simulation in both LS-DYNA and AUTODYN was performed with the same boundary conditions and the same types of finite elements. The boundary condition of zero normal velocity was specified for the air-filled space, the contour simulating the tubing was assumed to have solid and zero-normal-velocity boundary conditions, the water space was assumed to have the free-stream boundary. The boundary condition for the sample was specified as “no displacements normal to the sample plane throughout the 50 mm wide ring”, which ensured the same test area of the sample as in the actual tests. All the objects – sample, water, air, charge – were simulated by means of SOLID-type finite elements, the Euler mesh was used for water, air and charge, and Lagrange mesh – for the sample.

Mesh parameters (size, side proportions, density) were selected to minimize any effect upon the calculation results. In particular, characteristic size of the Euler mesh for water and air near the sample was ~4-5 mm, the size of the Lagrange mesh in the plane of the sample was 3.4 mm, the number of elements through the thickness of the sample was 6.

Equation of state for the water was polynomial. It was assumed that the pressure in liquid is never negative. This assumption is the simplest way to consider cavitation phenomena in liquid due to explosion processes. Air was modelled by the equation of ideal gas state. The explosion products were simulated using JWL equation. The factors and Chapman- Jouguet parameters for TNT were assumed. The tubing material was assumed to be absolutely rigid. The test sample material was treated as a quasi-isotropic material with linear elastic properties. The underwater explosion effect upon the sample was simulated in two stages. The first stage was the investigation of an explosion in the free infinite fluid in uni-dimensional (AUTODYN) or two-dimensional (LS-DYNA) formulation. In this formulation, the calculation was performed up to the moment corresponding to the shock wave approach to the sample. Then, this solution was exported into a 3D model including the sample, and the second stage of calculation followed.

Figs 8 and 9 show an example of comparison between computed time histories of radial and circumferential strains with similar time histories obtained experimentally for groups 1 and 3.

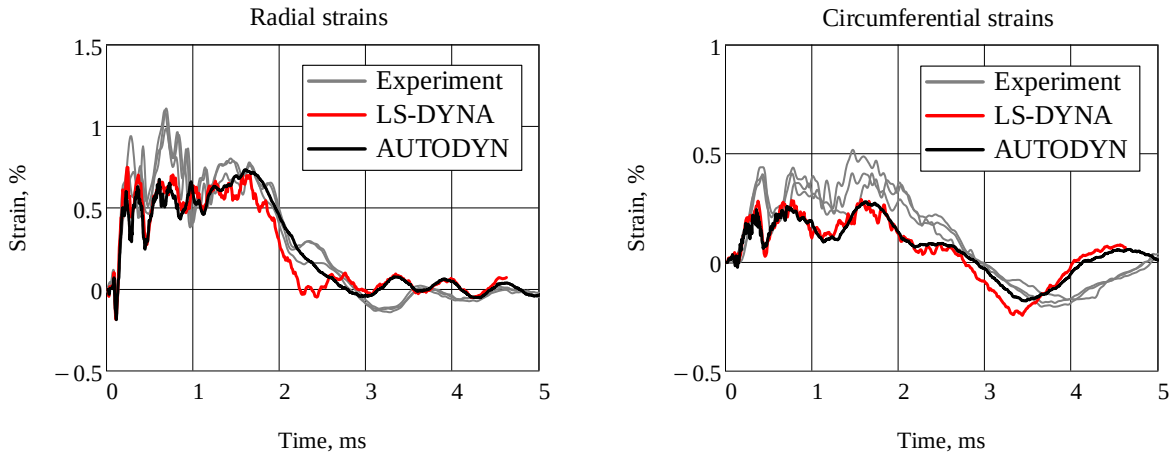

Figure 8. Comparison of simulations versus experiments. Group 1 samples. (Q=20 g, δ=5.94 mm)

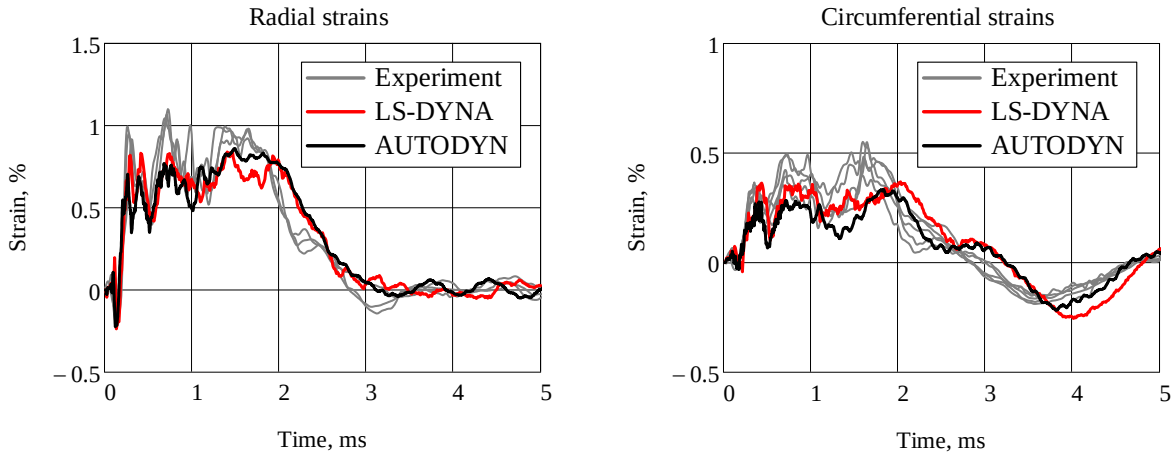

Figure 9. Comparison of simulations versus experiments. Group 3 samples. (Q=20 g, δ=5.28 mm)

It is seen that the computation results obtained by LS-DYNA and AUTODYN are in good agreement, and the computations show good qualitative and quantitative correlation with the experimental data.

Some deviation between computations and experiments can be put down to errors in actual sample thickness, discrepancy in coordinates of strains and locations of strain gauges (mostly affecting circumferential strains), errors in sample boundary condition simulations, ignoring of some orthotropy for materials under study, etc.

The elaborated computer models were used for a more detailed analysis of the stress-strain states of tested sample, in particular, membrane and bending deformations, radial and equivalent (von Mises) strains in the middle of the sample (Fig. 10) and at the sample support.

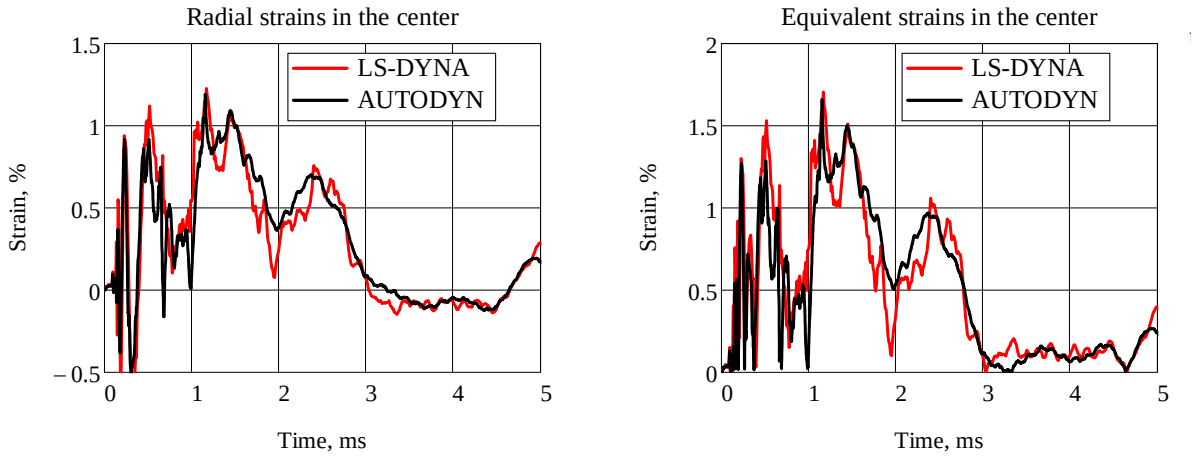

Figure 10. Computed time histories of radial and equivalent strains in the middle of sample. Samples of group 3. (Q=20 g, δ=5.28 mm)

In accordance with computations for the power intensity tentatively triggering ruptures of individual fibers, the levels of bending and membrane strains in the middle of test samples are practically the same. Bending strains are prevalent at the sample support. Since the sample material is assumed to be a quasi-isotropic material, it was interesting to compare the levels of equivalent strains in the middle part of samples. This comparison shows that the maximum value of the said strains is 10-20 % higher than at the sample support. Considering errors in computations versus experimental data, the equivalent strain in the middle portion reached 1.8 to 2.0% by the moment when fiber ruptures were initiated in the tests of group 2 and 3, correlating very well with ultimate tensile elongations of their materials. The obtained results suggest that in case of CFRP whose layup ensures the material quasi-isotropy and approximately equal tensile strains in various directions, the explosion resistance (based on fiber rupture initiation) can be evaluated in terms of the equivalent yield stress corresponding to the ultimate tensile elongation of material. For further analysis of the ultimate strain level it would be interesting to take into account the accumulation of material damage (in particular, binder failures) in the sample deformation process.

6. Conclusions

Results of experimental and computational studies conducted to investigate underwater explosion resistance of CFRP samples are presented. The samples were tested in the explosion test chamber of Krylov State Research Centre. The sample material damage was assessed versus two indications (criteria): rupture of individual fibers and through-thickness penetration (hole). The relative explosive charge mass (charge mass per unit effective area of sample related to sample surface mass) is taken as a measure of explosion effects causing a certain type of material damage. It is experimentally demonstrated that quadraxial carbon fabric samples show the best explosion resistance versus through-thickness penetration (hole generation) criterion due to better deformation characteristics as well higher interlaminar shear strength of the quadraxial carbon fiber plastic as compared with other materials under study.

Computer simulation models were developed and verified as applied to the test conditions to enable more detailed analysis of stress-strain states of tested samples. Based on the analysis of computational and experimental data it is demonstrated that by the moment when fibers start to rupture the equivalent strains in the middle of the test material samples, which have approximately the same ultimate tensile strength in different directions, show good correlation with the tensile elongation found in static tests.

It has been shown that the approach applied in this study to assess the explosion resistance of test samples based on the combined analysis of test data and computer simulations is an efficient tool revealing specific details of the deformation and damage process of tested samples.

References

[1] A.P. Mouritz. The effect of underwater explosion shock loading on the fatigue behaviour of GRP laminates. *Composites*, 26 (1):3-9, 1995.
[2] J. LeBlanc, A. Shukla. Dynamic response and damage evolution in composite materials subjected to underwater explosive loading: An experimental and computational study. *Composite Structures*, 92(10): 2421-2430, 2010.
[3] J. LeBlanc, A. Shukla. Response of E-glass/vinyl ester composite panels to underwater explosive loading: Effects of laminate modifications. *International Journal of Impact Engineering*, 38: 796-803, 2011.
[4] J. LeBlanc, A. Shukla. Dynamic response of curved composite panels to underwater explosive loading: experimental and computational comparisons. *Composite Structures*, 93: 3072-3081, 2011.
[5] A.I. Dulnev, E.A. Nekliudova. Resistance of GRP samples to non-contact underwater explosion. *Journal of Physics: Conference Series*, 919: 012003, 2017.
[6] R.C. Batra, N.M. Hassan. Response of fiber reinforced composites to underwater explosive loads. *Composites: Part B*, 38:448-468, 2007.
[7] A. Schiffer, V.L. Tagarielli. The Response of Circular Composite Plates to Underwater Blast: Experiments and Modelling. *International Journal of Impact Engineerin*, 52:130-144, 2015.
[8] *Explosion Blast Response of Composites*. ed. A. Mouritz and Y. Rajapakse. Woodhead Publishing, 2017.